Jeoloji Mühendisliği Dergisi / *Journal of Geological Engineering*
43 (2019) 155-186
DOI 10.24232/jmd.654888

Research Article / *Araştırma Makalesi*

Determination of the Deformability, Modulus Ratios and Anisotrophic Behavior of the Micaschists; A Case Study From Burgaz Dam Site, İzmir-Turkey

Mikaşistlerin Deformabilite, Modül Oranı ve Anizotropik Davranışlarının Belirlenmesi; Burgaz Baraj Sahasından (İzmir-Türkiye) Örnek Bir Çalışma

Serkan USLU[1] · Mehmet Yalçın KOCA[2]

[1]*Dokuz Eylül University, Graduate School of Natural and Applied Sciences, 35160, Buca-Izmir, Turkey*

[2] *Dokuz Eylül University, Eng. Faculty, Geol. Eng. Depart., 35160, Buca-Izmir, Turkey*

Geliş (*Received*): 07 Mayıs *(May)* 2019, Düzeltme (*Revised*): 05 Temmuz *(July)* 2019, Kabul (*Accepted*): 15 Ağustos *(August)* 2019

ABSTRACT

Base rock of the Burgaz dam in the eastern part of the city of İzmir consists of micaschists having different physical and mechanical properties due to weathering and fracturing. The first aim is to compute the amount of settlement and ultimate bearing capacity value of micaschist both in and beneath the cutoff zone by using the results of pressuremeter tests. In addition, data from in-situ and some laboratory tests, which were used in the establishment of the relations between elastic modulus of the micaschist rock mass (E_M) and uniaxial compressive strength (σ_c), E_M/E_{intact} ratios and RQD values. Comparison of in-situ and estimated rock mass deformation moduli by considering the RQD values was also performed. Pressuremeter tests indicate that for a dam with 115 m height and a base width of 58 m, the settlement will vary between 2.13 and 2.26 mm. The second aim of this work is to measure compression and shear wave velocities in order to obtain both the ratio of dynamic elastic modulus to Poisson′s ratio $(E/\nu)_{dynamic}$ and to compare $(E/\nu)_{dynamic}$ to $(E/\nu)_{static}$. Test results reveal a positive linear relation of $(E/\nu)_{dynamic} = (E/\nu)_{static} 0.968$. The sonic wave velocity of the micaschist is highly related to the testing direction. This study not only discusses the relationships between E_{static} and sonic wave velocity (V_p) and $E_{dynamic}$, but also the anisotropy effect arisen due to the schistosity planes with different orientations.

Keywords: Dam Structure, Micaschist, Pressuremeter Test, Settlement, Rock Material Classification, Anisotropy.

ÖZ

İzmir'in doğusunda yeralan Burgaz barajının temel kayacını ayrışma ve kırıklanma nedeniyle farklı fiziksel ve mekanik özelliklere sahip mikaşistler oluşturur. Bu çalışmanın birinci amacı, presiyometre deneylerinin sonuçlarını kullanarak hem cutoff zonunda hem de altında yeralan mikaşistlerin nihai taşıma güçlerini ve oturma miktarlarını hesaplamaktır. Buna ek olarak, bazı laboratuvar ve yerinde deneylerden elde edilen veriler, mikaşist kayaç kütlesinin elastisite modülü (E_M) ve sağlam kayanın tek eksenli sıkışma dayanımı (σ_c), E_M/E_i, oranları ve RQD değerleri arasındaki ilişkilerin kurulmasında kullanılmıştır. Mikaşist kayaç kütlesinin yerinde ölçülmüş elastisite modülü değerleriyle, RQD değerlerini dikkate alan tahmin edilmiş elastisite modülü değerleri karşılaştırılmıştır. Presiyometre

Yazışma Yazarı / *Correspondence:* yalcin.koca@deu.edu.tr

deney sonuçları, 58 m taban genişliğine ve 115 m yüksekliğe sahip bir baraj için oluşacak oturmaların 2.13 mm ile 2.26 mm arasında değişeceğine işaret etmektedir. Bu çalışmanın ikinci amacı; ultrasonik dalga hızlarından (V_p ve V_s) yararlanarak dinamik elastisite modülünün (E_{dyn}) Poisson oranına (ν) olan oranını, $(E/\nu)_{dyn}$ belirlemek ve $(E/\nu)_{dyn}$ ile $(E/\nu)_{statik}$ oranlarının karşılaştırılmasını yapmaktır. Deney sonuçları pozitif lineer bir ilişki vermiştir; $(E/\nu)_{dyn} = 0.968\ (E/\nu)_{statik}$. Mikaşistlerin sonik dalga hızının deney yönüyle oldukça ilişkili olduğu belirlenmiştir. Bu çalışma sadece E_{statik} ve sonik dalga hızı ilişkilerini tartışmaz, farklı konumlara sahip şistozite düzlemleri nedeniyle mikaşistlerde artan anizotropi etkisini de ele alır.

Anahtar Kelimeler: *Baraj yapısı, Mikaşist, Presiyometre deneyi, Oturma, Kaya Materyali Sınıflaması, Anizotropi.*

INTRODUCTION

Burgaz dam is a rock-fill dam constructed on Falaka River about 1 km north of Zeytinova town located in the Bayındır region of İzmir Province (Figure 1). The purpose of the dam is to supply irrigation water for a total land area of 35.68 km^2. The dam reservoir, which has a height of 115 m from the river bed and the dam body fill volume of 4.25 million m^3, is purposed to have the water storage capacity of 33 million m^3. Base rock of the Burgaz dam consists of micaschists. The behaviour of the micaschist rock mass is governed by the deformability of the base rock beneath the dam. The base rock of the dam must resist approximately 2 MPa total stress applied by the weight of dam itself and the strength of the rock must be sufficiently high because heavy pressures on the foundation of the dam will occur. This work gives the information on some physical and mechanical properties of the foundation rock beneath the dam structure, and about the settlement and bearing capacity values of the foundation rock. The design of the dam was based on these tests. Our study including a comprehensive investigation will hence be the first on the micaschists of the Menderes Massive in Turkey from the engineering geological point of view.

The values of elastic modulus (E_M) representing the micaschist rock mass were obtained from Menard pressuremeter tests (MPT) and these values were used in settlement and bearing capacity analyses. Comparison of in-situ and estimated rock mass deformation moduli by considering the RQD values is performed in this study. Comparison of the intact rock parameter such as E_i with those derived from in-situ tests is important in terms of the determination of relevant parameters for the dam design. Rock mass deformation modulus estimation by correlations considering RQD value has been performed since Coon and Merritt (1970). The correlations have included RQD (Gardner,1987; Kayabası et al., 2003; Zhang and Einstein, 2004; Kıncal and Koca, 2019). The estimated ratios considering the RQD values and in-situ ratios (E_{MPT}/E_i) based on the pressuremeter test results (E_{MPT}) and laboratory deformability tests are also compared. This comparison will indicate whether the elastic modulus representing the micaschist rock mass, which was used in the settlement analyses, is suitable, or not. On the other hand, the relationship between E_M and uniaxial compressive strength (σ_c) values is also investigated for the same purpose mentioned above in this study. Rowe and Armitage (1984) related the rock mass deformation modulus (E_M) for weak rocks deduced from a large number of field tests, and it was found as follows; $E_M = 0.215 \times \sqrt{\sigma_c}$, where σ_c is in MPa.

Another aim of this work is to obtain some strong correlations among sonic velocity and porosity, UCS and static modulus for the micaschists of the Menderes Massive. Empirical equations were then developed to predict the UCS, dynamic elastic modulus and dynamic Poisson's ratio based on the ultrasonic wave velocities. In order to determine the static modulus of the micaschist rock material, there are two ways proposed in this study; one of these

is to utilize from dynamic elastic modulus (E_{dyn}) and another one is from V_p. This paper is also intended to establish a relation between static and dynamic elastic moduli of the micaschist rock material as well as the relationship between static modulus (E_{static}) and V_p. The relationships between static and dynamic moduli and P-wave velocity were investigated by various authors in related literature (Eissa and Kazi, 1988; Heap et al., 2014; Najibi et al., 2015; Brotons et al., 2014; 2016).

UCS tests were performed with strain gauges and the values of static elasticity modulus (E_{static}) and Poisson′s ratio were determined from the stress-strain curves. Thus, empirical equations were also obtained between the UCS values and E_{static} and $(E/\nu)_{static}$, and $(E/\nu)_{static}$ and $(E/\nu)_{dynamic}$. These relationships mentioned above have been presented in the literature since Deere and Miller, 1966; Lama and Vutukuri, 1978; Al-Shayea, 2004; Uslu, 2017; Kadakcı Koca and Koca, 2018). Such correlations may provide a good estimation in some related engineering works. Correlations between sonic velocity, UCS and other physical properties and static modulus are important in terms of providing correct information for future exploration in the same or close areas, since a number of dams are planned to be built on the same schistous units belonging to the Menderes Massive in Aegean region by the General Directorate of State Hydraulic Works.

A comprehensive understanding of the anisotropy effect is necessary for a reliable design of engineering project such as dam construction (Behrestaghi et al., 1996; Singh et al., 2001; Nasseri et al., 2003). For this reason, P-wave velocity (V_p) measurements and compression tests were performed on the core specimens with different schistosity plane orientations. A review of the aforementioned work indicates that the maximum failure strength is either at $\alpha = 0°$ or $\alpha = 90°$ and the minimum value usually is around $\alpha = 30°$. The shape of the curve between UCS (σ_c) and α - angle reflects the anisotropy effect on the rock. In this work, loading was vertically applied on the core specimens with different schistosity plane orientations ($\alpha = 0 – 3°$, $\alpha = 28°$- $30°$, and $\alpha = 90°$). In addition, the relationship between UCS and sonic wave velocity was investigated previously in the literature for various rock types (Mc Cann et al., 1990 in Entwisle et al., 2005; Gupta and Seshagiri Rao, 1998; Sharma and Singh 2008; Andrade and Saraiva 2010). In this paper, a large number of ultrasonic pulse velocity tests were conducted on the micaschist intact core specimens obtained from ASK-1 borehole drilled in the Burgaz dam site.

GEOLOGY OF BURGAZ DAM SITE

Metamorphic rocks located in and nearby the Burgaz dam site have a simple tectonostratigraphy that consists of Paleozoic cover series and Pre-Cambrian core series which tectonically overlaid the cover series (Figure 1). Core series consist of homogenous garnet micaschists. Mineral composition of the garnet micaschist can be given as garnet-biotite-muscovite-plagioclase-quartz with accessory minerals of rutile, apatite and zircon. This rock contains 40% feldspar, 30% quartz, 20% mica (biotite+muscovite), 4 - 5% garnet and 1 – 2% other constituents. They display well developed lepidoblastic texture (Figure 2). The light brown color and weak schistosity are macroscopically characteristic features to recognize the schists at the Burgaz dam site.

Core samples obtained from the ASK-1 borehole have been examined petrographically. In the schist specimens, the interlocking fabric is created by the parallel to the sub-parallel arrangement of large platy minerals such as feldspar, mica, and quartz (Figure 2). In particular, strongly weathered schists tend to split into planes due to parallel orientation of

microscopic grains of mica, feldspars, quartz or other platy minerals (Figure 2). Traces of chemical decomposition such as discolouration with the alteration along linear elements were observed during the microscopic analyses of thin sections. The occurrence of defects which developed in the micaschists mechanically are sensitive along the entire length of the crystal rims. The defects include microfractures and mineral cleavages. As is to be expected, defects influence the ultimate strength of the micaschists and act as surface of weakness.

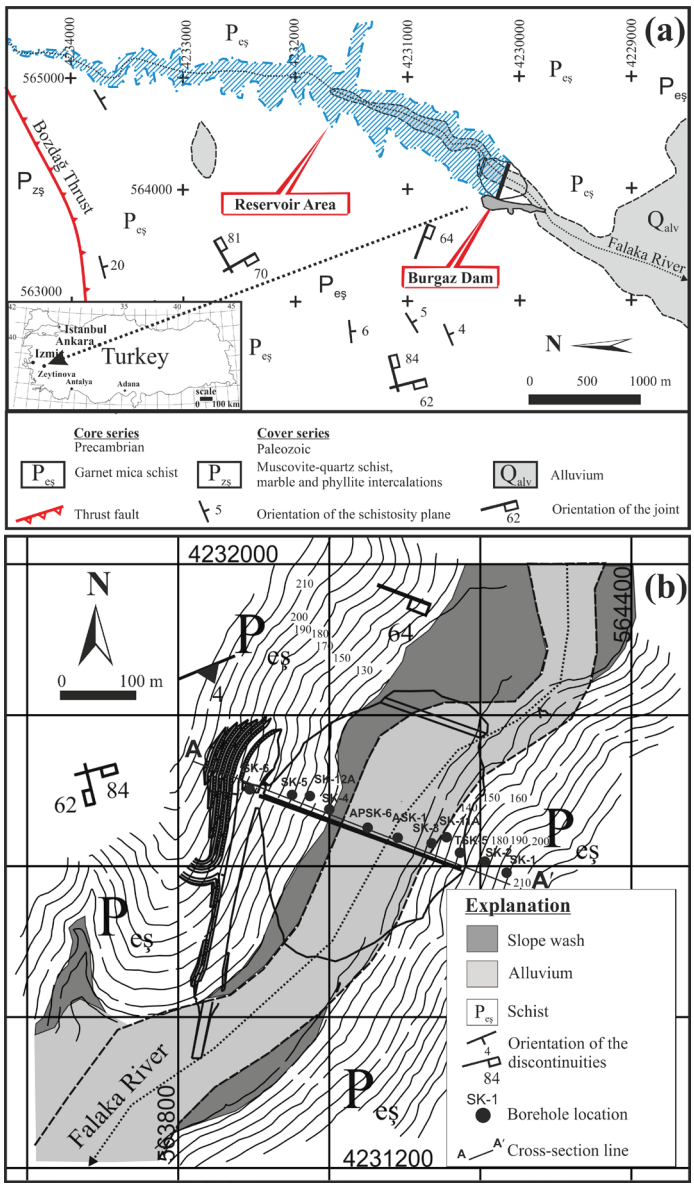

Figure 1. (a) Location and geological map of the Burgaz Dam Site and its nearby, (b) Geological map of the Burgaz dam site.

Şekil 1. (a) Burgaz Baraj Alanı ve yakın yöresinin lokasyonu ve jeoloji haritası, (b) Burgaz Baraj yeri jeoloji haritası.

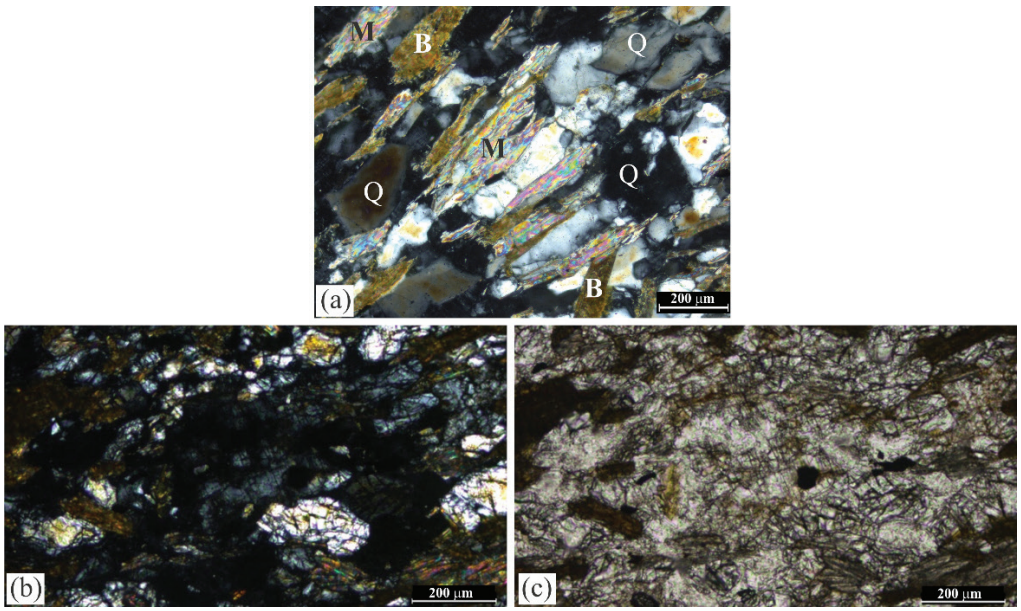

Figure 2. A view from the thin section of garnet micaschist (a) Q: quartz, M: muscovite, B: biotite, (Sample no: 1), (b) parallel nichol view, (c) cross nichol view.

Şekil 2. Granat mikaşistin ince kesitinden bir görünüm (a) Q: kuvars, M: muskovit, B: biyotit, (Örnek no:1), (b) paralel nikol görüntüsü, (c) haç nikol görüntüsü.

METHODS

The design of the dam was based on the results of pressuremeter tests. Design parameters such as limit pressure (P_L) and rock mass modulus (E_M) were evaluated using pressuremeter test results which can be used for the design of shallow and deep foundations in a fractured rock mass (Hughes, 2002; Tarnawski, 2004; Işık et al. 2008). 21 Menard pressuremeter tests were undertaken not only to assess bearing capacity and possible settlement at the base of the dam but also determine the depth of the cutoff level. Initially, the pressure applied was equivalent to 1 Atmosphere, increasing by 3 Atmospheres for each 2 m depth interval. The test results were evaluated for the rockfill dam with 115 m height and a base width of 58 m.

Both V_p and V_s measurements were performed using Proceq Pundit Lab device. V_p and V_s are the functions of elastic properties and rock density. Measurements therefore, provide the computing elastic modulus (E_{dyn}) and Poisson′s ratio (ν). These parameters are as follows; $E_{dyn} = \frac{\tilde{n} \times (3V_p^2 - 4V_s^2)}{\left(V_p^2/V_s^2\right) - 1}$, $\nu_{dyn} = \frac{\left(V_p^2/2V_s^2\right) - 1}{\left(V_p^2/V_s^2\right) - 1}$, where ρ is density of rock material.

Thus, the ratio of E_{dyn} to ν_{dyn} was computed for nine intact core specimens. In the present investigation, the ratios of $(E/\nu)_{dynamic}$ obtained from the measurements of sonic wave velocities were compared with the ratios of $(E_t/\nu)_{static}$ obtained from the direct static method. Sonic wave velocities of the micaschists were obtained by application of ultrasonic compression and shear waves pulses to the core specimen in accordance with ASTM test designation D 2845-08 (ASTM, 1990). Measurements were taken

along the axis of the core specimens and sonic wave velocities were determined from 50 core specimens. By considering the sonic velocity test on the rock specimens, the values of V_p and V_s of the core specimens under both dry and water saturated conditions were calculated. The velocities were measured on the core specimens with differently oriented schistosity planes of the rock such as parallel, inclined (28° - 30°) and vertical to the schistosity planes. On the other hand, the values of E_t (tangent elastic modulus) and Poisson′s ratio (ν) were calculated at 50% of the UCS from the stress versus strain curve of the rock. The values of UCS of the micaschist specimens were determined directly by testing 54 mm diameter NX size core specimens with a 1:2 dimensional ratio. The specimen was loaded until failure and stress-strain curve was recorded. Loadings were vertically applied to the schistosity planes (ASTM, 1992).

UCS tests were performed on that of 50 from 51 core specimens since the core specimen 47 was revoked due to the pre-existed joint. However, the deformability tests were solely performed on just 9 out of 50 intact core specimens. Furthermore, nine core specimens were taken from the core boxes to perform UCS tests under saturated conditions. The aim was to determine the strength reduction in saturated core specimens in proportion to the dry core specimens. In these tests, schistosity plane orientations were not considered. On the other hand, medium grained, slightly weathered blocks were extracted from the micaschist rock mass at the right bank of the dam reservoir to investigate the anisotropy effect. They were trimmed with their sides perpendicular to each other to facilitate coring at different inclinations, using a special frame fitted to the base of the laboratory drilling machine. Twenty-four specimens at different schistosity plane orientation angles (α = 0-3°, 28° - 30° and 90°) were cored from the three rock blocks. Thus, all laboratory tests were conducted on a total of 80 core specimens.

Engineering Geological Conditions of the Dam Site

ASK-1 drill-hole log contains some geological descriptions such as core recovery (CR%), RQD%, joint frequency (λ), and Lugeon test results (Figures 3 and 4). It is seen that the permeable and highly permeable levels have developed parallel to the schistosity planes with a nearly horizontal orientation (α < 10°), (Figure 3). The values of RQD along the borehole between 40 and 41.50 m, 51 and 52 m, 59 m and 63 m were determined to be less than 25% (Figure 5). These zones are of the property of very poor quality rock and permeable. Analysis of drilling data shows that pemeability inceases with poor – very poor rock quality.

Micaschists with poor quality were intersected between 31.5 m and 37.5 m, 39.5 m, 40 m – 41.5 m, 51 m – 52 m and 59 m – 63 m (Figure 4). The zones below 40 m depth were named as fractured zones in this work. Although a joint set was developed, permeability values under the cutoff level (21.0 - 28.5 m) were determined as 1.69×10^{-5} and 3.23×10^{-5} cm/s and the mean value was also computed as 2.02×10^{-5} cm/s (low permeable) due to its direction. While the test results of permeability are in interval between 3.23×10^{-4} cm/s and 1.69×10^{-5} cm/s near the foundation of the dam, under the depth of 60 m the test results are found to be an interval between 1.3×10^{-5} cm/s and 6.5×10^{-5} cm/s. This case indicates that the values of permeability decrease with the depth (Figure 3).

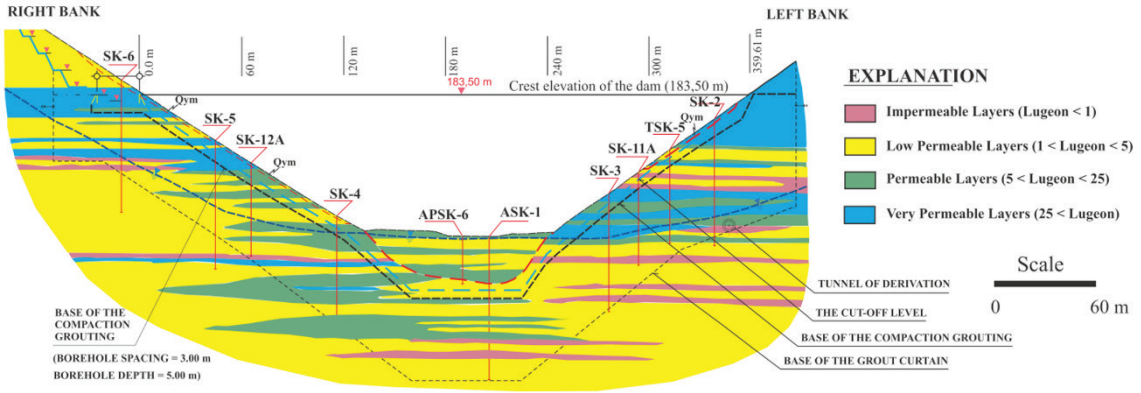

Figure 3. Zoning based on Lugeon values for the axis of Burgaz rock-fill dam (N72W).

Şekil 3. Burgaz kaya-dolgu barajının ekseni boyunca elde edilen Lugeon değerlerinin zonlaması (K72B).

Depth (m)	Zone	CR (%)	Spacing	λ (m^{-1})		RQD (%)	(m)	LU (Lugeon)		
28.5-31.5	-	100	-	-		35		Max:3.23 Min:1.89 Mean:2.02 n=5	Low Permeable	1-5
30-31.5				Mean	-	41				
31.5-37.5	I	100	Closely jointed S: 6-21cm	12	17	36				
37.5-39.5					5	91		6.39		5-25
39.5-40.0					14	41		Max:4.08 Min:1.24 Mean:2.9 n=4	Low Permeable	1-5
40.0-41.5					21	10				
41.5-44	II	100	Closely jointed S: 10-25 cm	7	4	60				
44-46					9	46				
46-50					5	53	48	11.92		5-25
50-51					11	35		3.03	Low Permeab.	1-5
51-52					20	24				
52-57	III	96	Closely jointed S: 20-25 cm		6	66	54	7.00		5-25
								2.87		1-5
57-59	IV	90	Very closely joint. S: 5-16 cm		13	42		Max:6.93 Min:5.02 Mean:5.70 n=3	Moderately Permeable	5-25
59-63		82			26	08				
63-85	V	100	Moderately jointed S: 22-96 cm	4	1-5	81	64	0.49	Very Low	< 1
							70	1.56		1-5
							75	0.70	Very Low Permeable	< 1
							76	24.75		5-25
							85	1.53		1-5

Figure 4. ASK-1 drill-hole log containing some engineering geological descriptions such as core recovery (CR%), RQD%, λ and Lugeon tests (Fractured zones: 40 – 41.5 m, 51 – 52 m and 59 – 63 m).

Şekil 4. Karot verimi (CR%), RQD% ve Lugeon deneyleri (Kırıklı zonlar : 40 – 41.5 m, 51 – 52 m ve 59 – 63 m) gibi mühendislik jeolojisi tanımlamaları içeren ASK-1 sondaj logu.

The maximum thickness of the alluvium in the river bed is 21.0 m (Figure 3). The cut off zone begins at the base of the alluvium (Figure 3). This zone is underlain by the moderately (WM) and highly weathered (WH) micaschists with quarzite lenses. Core advance into the WM and WH micaschist level is 53.5 m long (31.5–85 m). Intact rock cores were recovered from this zone. Some physical and mechanical properties of 50 micaschist core specimens are presented in Table 1.

Table 1. Some physical and mechanical properties of the micaschist core specimens obtained from the Burgaz dam site.

Çizelge 1. Burgaz Baraj alanından elde edilen mikaşist karot örneklerinin bazı fiziksel ve mekanik özellikleri.

Sample no	V_s-dry (m/s)	V_s-dry (m/s)	V_p-sat (m/s)	γ_{dry} (kN/m^3)	γ_{sat} (kN/m^3)	n %	σ_c-dry (MPa)	σ_c-sat (MPa)	E_t (GPa)
1	1180	1710	2346	24.70	25.60	9.72	20.30	-	-
2	1195	1758	2350	25.10	26.00	8.19	24.80	-	-
3	1136	1890	2536	25.10	25.90	8.07	25.40	-	-
4	1040	1890	2510	24.70	25.60	9.23	22.80	-	-
5	1176	2136	2744	25.50	26.20	6.59	32.60	-	-
6	1174	2214	2880	25.40	26.10	7.05	33.20	-	-
7	1317	2092	2714	25.20	25.90	7.75	29.80	-	5.98
8	1155	2100	2658	26.30	26.80	4.85	38.80	-	-
9	1200	1906	2508	25.40	26.10	7.10	28.20	-	-
10	1392	2047	2672	26.10	26.60	4.79	35.00	-	-
11	1305	2510	3346	27.20	27.40	1.95	41.50	-	-
12	1292	2486	3281	26.90	27.20	3.18	42.80	-	-
13	1480	2680	3495	27.00	27.20	1.98	46.20	-	-
14	1424	2094	2590	26.10	26.50	4.80	38.20	-	-
15	1469	2160	2704	26.00	26.50	4.94	39.00	-	-
16	1450	2544	3330	26.90	27.10	2.01	42.60	-	10.80
17	1452	2640	3379	26.80	27.10	2.80	40.60	32.50	-
18	1706	2820	3694	26.80	27.00	2.01	51.40	-	17.86
19	1728	3084	3886	26.90	27.10	1.82	47.40	-	-
20	1605	2360	3160	26.80	27.00	2.68	36.70	30.40	-
21	1728	2741	3544	27.00	27.20	1.97	48.00	39.00	13.00
22	1633	2402	3184	26.90	27.20	3.15	33.60	-	-
23	1637	2444	3228	26.90	27.20	3.26	41.90	-	-
24	1820	3200	3746	27.00	27.20	1.81	45.00	-	20.59

Table 1. Continued.

Çizelge 1. Devam ediyor.

25	2318	3800	4750	27.20	27.40	1.84	60.40	50.70	-
26	2386	3560	4510	27.20	27.40	1.79	61.90	-	-
27	1645	2610	3400	26.30	26.80	4.86	43.40	-	-
28	1730	2704	3400	27.10	27.30	2.60	46.50	-	-
29	2419	3840	4802	27.00	27.20	1.75	58.50	-	-
30	2421	3780	4608	27.30	27.50	1.68	66.80	-	-
31	1920	3240	3900	26.90	27.10	1.92	55.00	-	19.00
32	1728	2742	3442	27.10	27.30	2.18	44.80	-	-
33	1680	2780	3005	26.20	26.60	4.20	40.48	-	15.52
34	1504	2212	2984	26.50	26.90	4.53	31.00	-	-
35	1290	2144	2873	25.50	26.20	6.51	30.10	-	-
36	1580	2508	3217	26.10	26.60	4.63	34.90	-	-
37	1462	2150	2803	25.40	26.10	6.66	26.00	-	-
38	2130	4020	4918	27.10	27.20	1.59	78.10	-	-
39	2090	3850	4504	27.40	27.50	1.44	56.2	-	27.12
40	1350	3812	4742	27.30	27.40	1.69	67.30	-	-
41	1815	3128	3792	27.00	27.20	1.78	62.40	-	-
42	2153	3987	4889	27.00	27.10	1.64	69.80	61.00	-
43	1896	3100	3868	27.00	27.20	2.01	70.20	63.10	-
44	2085	3790	4449	26.90	27.10	2.08	65.00	-	-
45	2819	4208	5090	27.30	27.40	1.53	79.60	-	-
46	2460	3904	4802	27.30	27.50	1.74	71.60	-	36.40
48	2504	4106	5156	27.40	27.50	1.43	76.80	-	-
49	2798	4442	5240	27.50	27.60	1.11	81.80	-	-
50	2378	4100	4870	27.30	27.50	1.54	72.00	-	-
51	2860	4540	5312	27.50	27.60	1.15	80.50	-	-
$\bar{X}$± SD	1752.32 ± 500.93	2880.74 ± 807.4	3636 ± 899.3	26.56 ± 0.08	26.90± 0.056	3.55± 2.40	48.34 ± 17.4	46.12± 14.24	18.40 ± 9.153

σ_c values of the 39 core specimens (78% of all core specimens) recovered from depths between 40-47 and 63-67 m, and 73-85 m were examined under two groups; *i)* $\sigma_c > 50$ MPa, $2000 < V_p < 4000$ m/s (26% of all core specimens), *ii)* $15 < \sigma_c < 50$ MPa, $2000 < V_p < 4000$ m/s (52% of all core specimens), (Table 2 and Figure 5).

Table 2. The degree of weathering and corresponding ultrasonic velocities for the micaschists from the Burgaz Dam site.

Çizelge 2. Burgaz Baraj sahasındaki mikaşistlerin ayrışma dereceleri ve onlara karşılık gelen ultrasonik ses dalgası hızları.

Weathering state	Number of intact core specimens	UCS (MPa)	Ultrasonic velocity (m/s)		α-ratio $\left(\frac{V_p \text{ saturated}}{V_p \text{ dry}}\right)$ "For all data"
			Dry (average)	Saturated (average)	
WS	6 (12%)	$\sigma_c > 50$	4236.0	5097.6	1.210
WM	13 (12%)	$\sigma_c > 50$	3576.7	4374.8	1.223
WH	26 (52%)	$15 < \sigma_c < 50$	2498.8	3109.0	1.289
WC	5 (10%)	$15 < \sigma_c < 50$	1830.8	2450.0	1.338

Explanation: WS: Slightly weathered, WM: Moderately weathered, WH: Highly weathered, WC: Completely weathered.

While the micaschist core specimens including the first group (WH – WM) were classified as "moderately weathered, strong rock", those included in the second group were classified as "slightly weathered (WS), moderately strong rock" (Figure 5). On the other hand, values of the five core specimens (10% of all core specimens) recovered from depths between 28.5 and 37 m were found to be in the range between 20 MPa and 30 MPa (Figure 5). In addition, V_{pdry} values of these core specimens (WC) were determined to be less than 2000 m/s. These core specimens were classified as "completely weathered, moderately strong rock" (Table 2 and Figure 5).

Anisotropic Behaviour of the Micaschists

V_p and UCS tests were conducted on the core specimens as shown in Figure 6. V_p-values were measured on the core specimens with differently oriented schistosity planes such as parallel (α = 0 - 3°) to the schistosity planes, inclined (28° - 30°) to the schistosity planes, and vertical (α = 90°) to the schistosity planes, under dry and saturated conditions, respectively (Figure. 6). After the processes mentioned above, the (V_{psat} /V_{pdry}) ratios were computed for the core specimens and shown in Table 3.

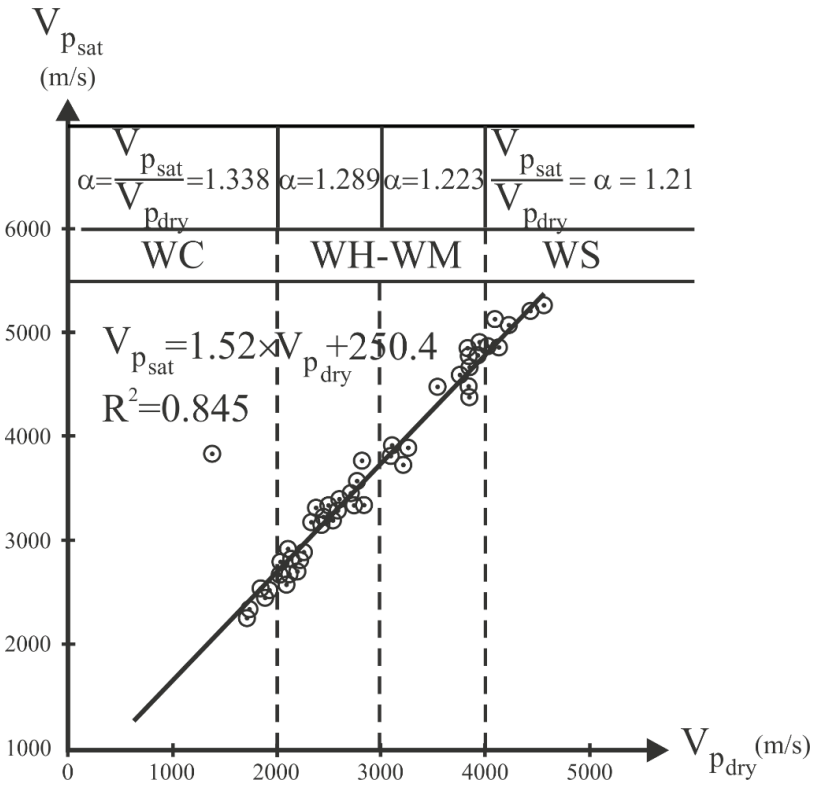

Figure 5. Relationships between ultrasonic wave velocities under dry and water saturated conditions and the values of α-ratio (V_{psat}/V_{pdry}).

Şekil 5. Kuru ve suya doygun şartlarda ultrasonik ses dalgası hızlarıyla α-oranı (V_{psat}/V_{pdry}) değerleri arasındaki ilişkiler.

V_p-values obtained parallel or nearly parallel to the schistosity planes (α = 0 – 3°) were the highest as compared to other orientations in both dry and water saturated conditions. V_p-values acquired at 28° – 30° were higher than those vertical to the schistosity planes (α = 90°) in dry condition, while in water saturated condition, V_p values were obtained as close to each other for both α = 28° – 30° and (α = 90°), (Table 3). P-wave velocities obtained for α = 28° – 30° are higher than those obtained for α = 90° in dry condition. On the other hand, in saturated condition, the mean values of P-wave velocities for anisotropy angles both α = 28° – 30° and α = 90° are nearly obtained in the same level. As a result, it is determined that the V_p value decreases as α-angle increases. On the other hand, as the α-angle decreases, the (V_{psat}/V_{pdry}) ratio increases. A similar trend was observed for quartz mica schists by Zhang et al. (2011). The difference between the mean values of the wave-velocities measured under saturated and dry conditions (V_{psat}/V_{pdry}) and the percent of increasing the velocity were determined for the various α-angles (Table 3). It is determined that as α-angle increases, the difference between V_{psat} and V_{pdry} also increases.

Table 3. P – wave velocities of slightly weathered mica schists core specimens (Increasing the velocity for (V_{psat}-V_{pdry}): For α = 0 - 3°: 894 m/s, for α = 28° – 30°: 1141 m/s, for α = 90°: 1770 m/s).

Çizelge 3. Az ayrışmış mikaşist karot örneklerinin P-dalga hızları (Artan (V_{psat}-V_{pdry}) hız : α = 0 - 3° için 894 m/s, α = 28° – 30° için 1141 m/s, α = 90° için 1770 m/s).

α-angle		P-wave velocities (m/s) Dry (V_{pdry})	Saturated (V_{psat})	V_{psat}/V_{pdry} ratio
		Increasing the velocity		
0 - 3°	Maximum	4590	5360	
	Minimum	3946 →	4915	1.21
	Average	4232 ± 224	5126 ± 190.5	
	N: 8			
	(V_{pdry}) (V_{psat})	894 (21.2%)		
28° - 30°	Maximum	2262		
	Minimum	1860 →	3652	
	Average	2001±128.4	3142±256.5	1.57
	N: 8	2780		
	(V_{psat}) (V_{pdry})	1141 (57%)		
90°	Maximum	1640	4264	
	Minimum	890 →	2006	
	Average	1320±233.7	3090±663.9	2.34
	N: 8			
	(V_{psat}) (V_{pdry})	1770 (134%)		

N: number of test, α-angle: Anisotropy angle (It is defined as an angle between the applied compressive loading and the schistosity plane orientation).

It was determined that the ratio is the largest (2.34) for α = 90° and the smallest (1.21) for α = 0–3° in this study. When P–wave propagates along the schistosity plane (α=0-3°), the presence of water makes a slight influence on the wave velocity (V_{psat} /V_{pdry}= 1.21). On the other hand, when P–wave propagating at the vertical position to the schistosity planes (α = 90°), the presence of water significantly increased the wave velocities (V_{psat} /V_{pdry}= 2.34). UCS test results of the micaschist core specimens with differently oriented schistosity planes in both dry and water saturated conditions are presented in Table 4.

Figure 6. The relationship between loading direction and schistosity planes (α: anisotropy angle).

Şekil 6. Yükleme yönüyle şiştozite düzlemler arasındaki ilişki (α: anizotropi açısı).

Table 4. UCS – test results of the mica schist core specimens with differently oriented schistosity planes in both dry and water saturated conditions.

Çizelge 4. Kuru ve suya doygun şartlardaki farklı şistozite düzlem konumlu mikaşist karot örneklerinin tek eksenli basınç deneyi sonuçları.

α - angle					
90°		**0 – 3°**		**28° – 30°**	
σc – dry, MPa	σc – sat MPa	σc – dry, MPa	σc – sat MPa	σc – dry, MPa	σc – sat MPa
75.0	54.2	61.6	35.0	45.0	18.5
74.2	55.4	60.4	34.0	38.6	16.2
70.0	50.6	57.0	32.6	43.6	17.0
78.0	56.3	55.6	31.0	29.0	14.8
74.3 ± 3.30	54.1 ± 2.50	58.6 ± 2.81	33.1 ± 1.82	39.0 ± 7.24	16.6 ± 1.54
*N: 4	N: 4	N: 4	N: 4	N: 4	N: 4
$\sigma_{cdry}/\sigma_{csat}$= 1.37		$\sigma_{cdry}/\sigma_{csat}$= 1.77		$\sigma_{cdry}/\sigma_{csat}$= 2.35	

*N: Number of test

In both dry and saturated conditions, the highest UCS values were obtained from the uniaxial compression tests when loading is perpendicular to the schistosity planes (α = 90°). On the other hand, the smallest ones were obtained from the tests when loading is inclined to the schistosity planes (α = 28-30°). The relationships between the $\sigma_{cdry}/\sigma_{csat}$ ratio and α - angle were examined in detail (Figure 7). The largest and smallest $\sigma_{cdry}/\sigma_{csat}$ ratios are found as 2.35 (α = 28°-30°) and 1.37 (α = 90°), respectively. For this reason, the curve acquired from the variation of $\sigma_{cdry}/\sigma_{csat}$ ratio with α-angle displays a reverse V – shape (Λ - shape). Variation of the UCS – mean values with α-angle in both dry and saturated conditions was also examined to better characterize the anisotropy effect of the mica schists (Figure 8). The curves obtained from the variation of the UCS - mean values with α - angle display V – shape (Figure 8). Besides, the V-shape may result from only three conditions for the plane direction being considered. The anisotropy behavior of micaschists is clearly shown in UCS test results, i. e. the ratio of $\sigma_{cdry}/\sigma_{csat}$ varies with the α - angle between the applied compressive loading and the schistosity plane orientation. In dry condition, while the UCS – mean value was found as 74.3 MPa when loading during the compression tests was perpendicular to the schistosity planes (α = 90°), it was found as 39.0 MPa when loading was inclined to the schistosity planes (α = 28°- 30°). In saturated condition, these values were found as 54.1 MPa and 16.6 MPa, respectively (Figure 8).

While in the relationship between α-angle and V_p, the values of V_p in saturated condition were obtained higher than those in the dry condition. In the relationship between α-angle and UCS–values, UCS–values were obtained as higher than those in water saturated condition (Figure 8). While the V-shape from the relationship between α-angle and UCS was acquired, the relationship between α-angle and the curve of V_p did not display such a trend (Figure 8). As expected, they do not agree with each other.

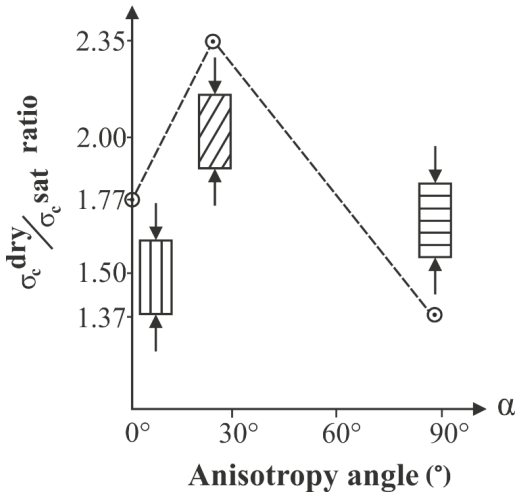

Figure 7. Variation of $\sigma_{cdry}/\sigma_{csat}$ ratio with α-angle (anisotropy angle).

Şekil 7. Anizotropi açısıyla (α)−$\sigma_{cdry}/\sigma_{csat}$ oranı değişimi.

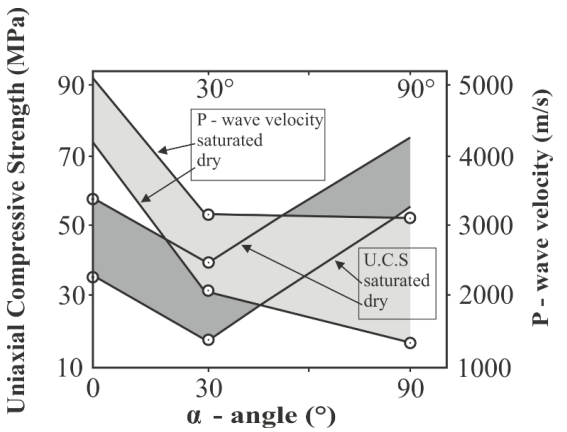

Figure 8. Relationships between α-angle and uniaxial compression strength, and P–wave velocity for the micaschist core specimens with different schistosity planes in both dry and water saturated conditions.

Şekil 8. Kuru ve suya doygun şartlardaki farklı konumlu şiştozite düzlemli mikaşist karot örnekleri için anizotropi açısı (α), Tek Eksenli Basınç Dayanımı ve P-dalga hızı ilişkileri.

Determination of the Deformability and Modulus Ratios of the Micaschists

In order to determine the modulus ratios, nine deformability tests were performed on the intact core specimens (Figure 9). While the UCS values were determined in a range between 29.8 MPa and 71.6 MPa, the values of E_t were also determined in a range between 5.98 GPa and 36.4 GPa (Table 5). This large variability can be attributed to various weathering grades, not to rock anisotropy, because loadings in all tests were vertically applied on the schistosity planes. Deformability is classified into five categories as proposed by the IAEG (Anon, 1979). According to this classification, high deformability is less than 15×10^3 MPa, low deformability is greater than 30×10^3 MPa. Except for the core specimens number 7, 16 and 21, micaschists were classified as moderate deformable (15.52×10^3 MPa $\leq E_t \leq 27.12\times10^3$ MPa). The values of of the core specimens number 7, 16 and 21 were found as 5.98, 10.82 and 13.0 GPa, respectively (Figure 9). They were classified as "high deformable rock". The elastic modulus value of the core specimen number 46 was determined as a low deformable category ($E_t > 30\times10^3$ MPa), (Table 5). The ultimate deformation (strain at failure) is considerably high in weathered micaschist which appears as an outcome of a more ductile behaviour of the material. The higher values of σ_c, the slope of the ascending branch of the stress–strain diagram, in comparison with the slope exhibited by weathered mica schists (Figure 9). Their results with the modulus ratios are given in Table 5.

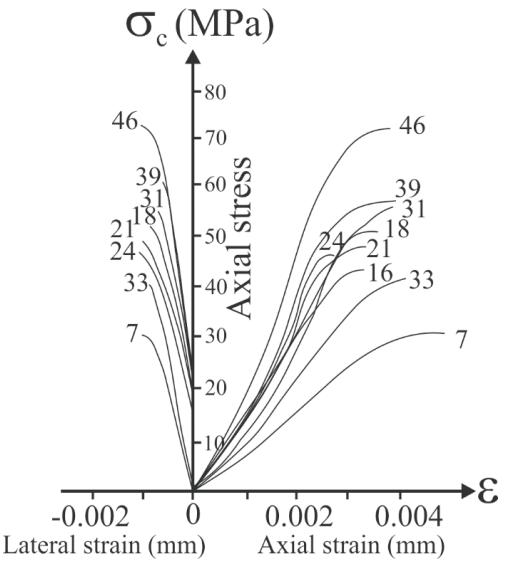

Figure 9. The axial and diametric stress-strain curves of the micaschists.

Şekil 9. Mikaşistlerin eksenel ve çapsal gerilme-deformasyon eğrileri.

According to the engineering classification of intact rocks suggested by Deere and Miller (1966), except the core specimen 7, micaschists were classified as "average modulus ratio" and "moderately strong rocks". The specimen number 7 was classified as "average modulus ratio" and "weak rock". According to the proposed method by Türk and Dearman (1983), micaschists were classified as "moderately deformable and moderately strong and strong rocks" (Figure 10). The specimens 7 and 46 were classified as "moderately strong and very deformable" and "strong and slightly deformable rock", respectively (Figure 10). In this work, the values of σ_c and E_t/v were determined in the ranges between 29.8 MPa and 71.6 MPa, and 34.76 and 145.6 GPa, respectively.

Table 5. Deformability test results and modulus ratios for the micaschist core specimens.
Çizelge 5. Mikaşist karot örnekleri için deformabilite deney sonuçları ve modül oranları.

Sample no	n%	*σc* (MPa)	ν	E_t (GPa)	*Et/óc*	*Etv* (GPa)
7	7.75	29.8	0.17	5.98	201	34.76
16	1.92	42.6	0.26	10.82	254	41.61
18	2.01	51.4	0.22	17.86	374	81.20
21	1.97	48.0	0.17	13.00	271	76.47
24	1.81	45.0	0.27	20.59	458	76.30
31	1.92	55.0	0.18	19.00	345	105.66
33	4.20	40.5	0.20	15.52	383	77.60
39	1.44	56.2	0.30	27.12	482	90.40
46	1.74	71.6	0.25	36.40	508	145.6
X ± S.D	2.75±2.03	48.89±11.74	0.22±0.04	18.47±9.04	363.96±107.2	81.06±32.8

From the graph presented in Figure 10, it is seen that the UCS values increase as the ratios of ($\frac{E_t}{\nu}$) increase. UCS test results, the values of E_t and ν, modulus ratios ($\frac{E_t}{\sigma_c}$) and the value of ($\frac{E_t}{\nu}$) for each test are given in Table 5. While the value of modulus ratio of ($\frac{E_t}{\sigma_c}$) was found to be in a range between 200.6 and 508.3, the ratio of ($\frac{E_t}{\nu}$) was found to be in a range between 34.76 GPa and 145.6 GPa with a mean value of 81.06 ± 32.8 GPa (Table 5). Logarithmic, power and linear regression analysis between σ_c and values for the micaschists were performed and $\frac{E_t}{\nu}$ the Equations 1, 2 and 3 were obtained.

$$\text{Log } \sigma_c = \log 5.3936 + m \times \log \left(\frac{E_t}{\nu} \right) \quad (1)$$

Where "m" is slope of the plot.

Power and linear regression analyses between ($\frac{E_t}{\nu}$) and values for the micaschists with medium elastic modulus ratio were performed and then Equations 2 and 3 were obtained. If the correlation coefficients obtained from both analyses are considered, it is seen that the coefficient acquired from the power regression analysis is less than that of the linear regression analysis.

$$\sigma_c = 5.3936 \times \left(\frac{E_t}{\nu} \right)^{0,5047} \qquad R^2 = 0.81 \quad (2)$$

$$\sigma_c = 0.3331 \left(\frac{E_t}{\nu} \right) + 21.899, \qquad R^2 = 0.86 \quad (3)$$

Comparison of the test results from the Burgaz dam site with those from Selçuk-İzmir (Elçi, 2003) was also performed in this study. For this, test results on WS-micaschists from Selçuk-İzmir and WM-WH micaschists from the Burgaz dam site-İzmir were plotted all together in Figure 10. When weathering grade increases, both strength and (E_t/v) values decrease along a straight line which is represented by the equation in Figure 10. While the slope of the line given in Equation 4 is 0.3331, in Equation 5, it is 0.1779. The slope of line decreased nearly two times (Figure 10). However, micaschist test results follow a power law;

$$\sigma_c = 7.5393 \times \left(\frac{E_t}{\nu} \right)^{0,4244} \qquad R^2 = 0.89 \quad (4)$$

$$\sigma_c = 0.1779 \left(\frac{E_t}{\nu} \right) + 33.691 \qquad R^2 = 0.84 \quad (5)$$

According to the Equations 4 and 5, WM and WS micaschists with medium elastic modulus ratio gave reasonably acceptable power and linear relations, respectively.

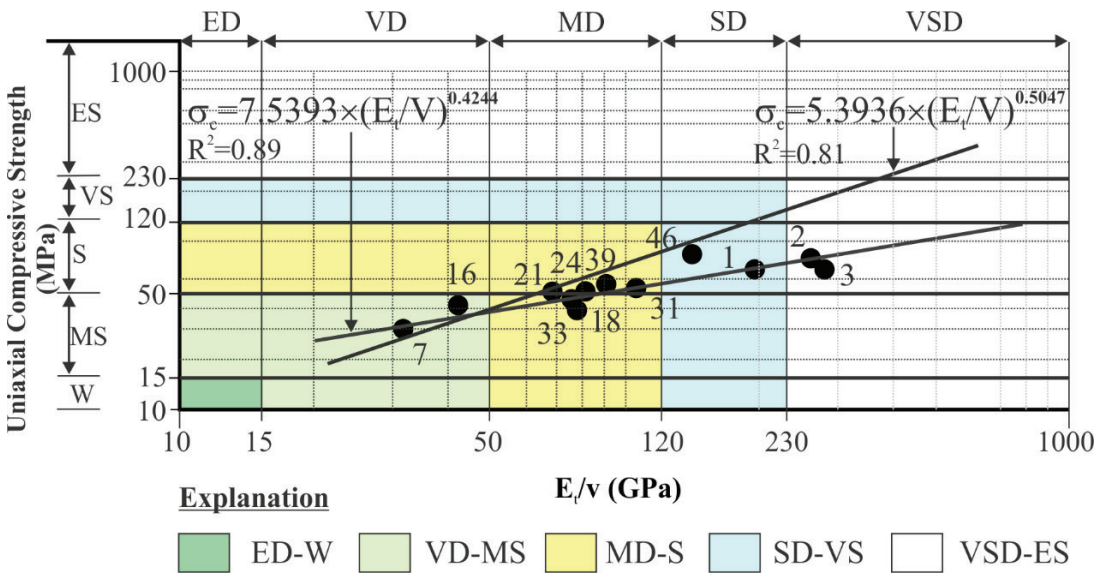

Figure 10. Graphical presentation of the relationship between $\left(\frac{E_t}{\nu}\right)$ ratio and uniaxial compressive strength (7, 18, 24, 31, 33 and 39: from the Burgaz dam site, 1, 2, and 3: Selçuk-İzmir, n% ≤ 1.6, $\sigma_c \geq$ 76 MPa, = 50 - 70 GPa). Engineering classification of intact micaschist core specimens (W: Weak, MS: Moderately strong, S: Strong, VS: Very strong, ES: Extremely strong, ED: Extremely deformable, VD: Very deformable, MD: Moderately deformable, SD: Slightly deformable, VSD: Very slightly deformable).

Şekil 10. $\left(\frac{E_t}{\nu}\right)$ *oranıyla tek eksenli basınç dayanımı ilişkisinin grafiksel sunumu (7, 18, 24, 31, 33 ve 39: Burgaz barajı sahasından, 1, 2, ve 3: Selçuk-İzmir'den, n% ≤ 1.6,* $\sigma_c \geq$ *76 MPa, = 50 - 70 GPa). Taze mikaşist karot numunelerinin mühendislik sınıflaması (W: Wayıf, MS: Orta dayanımlı, S: Dayanımlı, VS: Yüksek dayanımlı, ES : Çok yüksek dayanımlı, ED: Aşırı derecede deforme olabilen, VD: Çok deforme olabilen, MD: Orta derecede deforme olabilen, SD: Az deforme olabilen, VSD: Çok az deforme olabilen).*

Relation Between $(\frac{E}{\nu})_{dynamic}$ and $(\frac{E_t}{\nu})_{static}$ for the Micaschists

V_p and V_s velocities were measured to determine the ratio of $(E/\nu)_{dyn}$ for nine intact core specimens. Results of the measurements $(E/\nu)_{dyn}$ and ν are presented in Table 7. The ratios of $(E_t/\nu)_{static}$ for the same core specimens are also presented in this table. The results show that $(E/\nu)_{dyn}$ is greater than $(E_t/\nu)_{static}$ (Table 6). The graph of $(E/\nu)_{dyn}$ versus $(E_t/\nu)_{static}$ is drawn on a log-log paper (Figure 11) and the relation given in Equation 6 was obtained;

$$(\frac{E}{\nu})_{dyn} = 1.2707\ (\frac{E_t}{\nu})^{0.968}_{static} \qquad R^2 = 0.96,\ n = 9 \quad (6)$$

The plot of test results indicates that there are two points to consider; *a)* When $(E_t/\nu)_{static}$ is high, as for the moderately strong micaschists, $(E/\nu)_{dyn}$ is also high and values are greater than $(E_t/\nu)_{static}$. *b)* The decrease in $(E_t/\nu)_{static}$ value shows a corresponding decrease in $(E/\nu)_{dyn}$. The values of E_t and ν from the laboratory tests performed under dynamic and static conditions were found to be different from one another. For this reason, both the values of E_t and ν were considered in which the relations were examined. Figure 11 shows the log-log scale plot of "Average Modulus Ratio" and $(E/\nu)_{dyn}$ against $(E_t/\nu)_{static}$ for the weathered micaschists from the Burgaz dam

site. It is interesting to note that the test results of the micaschists gave a power relation of $y=ax^b$ [$(\frac{E}{\nu})_{dyn} = 1.2707 \times (\frac{E_t}{\nu})^{0.968}$, $R^2= 0.96$], as a linear relation: [$(\frac{E}{\nu})_{dyn} =79.192 \ln (\frac{E_t}{\nu})_{static}–252.14$ on a log-log scale, $R^2= 0.88$].

Relationships between the static and dynamic moduli and V_p were also investigated in this study. As known, the dynamic modulus (E_{dyn}) is generally higher than the static, but there are instances where the opposite is true. The higher the E_t, the greater the agreement between the static and dynamic values is (Eissa and Kazi, 1988). The relationships between the static and dynamic moduli for different types of rocks and ranges of values proposed by various authors (Brotons et al. 2016; Christaras et al. 1994; Eissa and Kazai, 1998) are summarized in Table 7. In addition, various correlations between E_{static} and E_{dyn} moduli were proposed by various authors (Figure 12). They have been obtained from rocks whose dynamic modulus varied between 5 and 130 GPa, and including rocks of igneous, sedimentary and metamorphic origins (all rock types). k-ratio (E_{dyn} / E_{static}) has been used in their works by several authors (Al-Shayea, 2004; Martinez et al., 2012; Brotons et al., 2014; 2016) as well as the current study. In Figure 12 the line of slope 1:1 from the origin, represents the points where k=1, so that the values of k>1 are located to the right of that line (Figure 12). All of the curves in Figure 12 are located in the right of the diagonal line, indicating k>1 values.

Table 6. Results of the measurements of P and S ultrasonic wave velocities and the values of $(\frac{E_t}{\nu})_{static}$ and $(\frac{E}{\nu})_{dynamic}$.

Çizelge 6. P ve S ultrasonik dalga hız ölçüm sonuçlarıyla $(\frac{E_t}{\nu})_{static}$ ve $(\frac{E}{\nu})_{dynamic}$ değerleri arasındaki ilişkiler.

Sample No	Vs_{dry} (m /sec)	Vp_{dry} (m /sec)	$\left(V_p^2/V_s^2\right)$	ñ (kg/m^3)	ν	E_{dyn} (GPa)	$\frac{E_{dyn}}{\nu}$ (GPa)	$\frac{E_{stat}}{\nu}$ (GPa)
7	1317	2092	2.52	2.52×10^{-3}	0.172	6.19	35.99	34.8
16	1450	2544	3.07	2.69×10^{-3}	0.260	14.25	54.80	41.6
18	1706	2820	2.73	2.68×10^{-3}	0.210	18.90	90.10	81.2
21	1728	2741	2.51	2.70×10^{-3}	0.180	18.86	75.44	72.2
24	1820	3200	3.10	2.70×10^{-3}	0.263	22.60	85.90	76.3
31	1920	3240	2.84	2.69×10^{-3}	0.230	24.50	106.4	105.6
33	1680	2780	2.74	2.62×10^{-3}	0.210	17.90	85.40	77.6
39	2090	3850	3.39	2.74×10^{-3}	0.290	30.50	104.6	90.4
46	2378	4100	2.97	2.75×10^{-3}	0.250	42.00	168.00	145.6

Explanation: ñ: Density, ν: Poisson′s ratio, V_s and V_p: Sonic wave velocities.

Table 7. Relationships between E_{static} and $E_{dynamic}$ moduli proposed by various authors.

Çizelge 7. Farklı yazarlar tarafından önerilen E_{static} ve $E_{dynamic}$ modülleri arasındaki ilişkiler.

Reference	Relationship	R^2	E_{dyn} (GPa)	Rock type
Eissa and Kazi (1988)	$E_{static} = 0.74 \times E_{dyn} - 0.82$	0.70	5 – 130	All types
Christaras et al. (1994)	$E_{static} = 1.05 \times E_{dyn} - 3.16$	0.99	25 – 110	All types
Brotons et al. (2016)	$E_{static}=11.531\times \rho_{bulk}^{-0.457} \times E_{dyn}^{1.251}$	0.99	5 – 80	All types
The current study	$E_{static} = 0.8764 \times E_{dyn} - 0.58$	0.97	5 – 30	Mica schist

The evolution of the k-parameter with the modulus for each curve can be seen in Figure 12. The k-values obtained in this study vary from 1.06 to 1.45. The mean value is found as 1.198 ± 0.126. The values obtained by the other authors are between 0.85 and 1.86 (King, 1983; Vanheerden, 1987; Eissa and Kazi,1988). The k-values obtained in this study generally agree with the findings of the other authors.

The parameter required in the equations (V_p) is easily obtained. It simplifies simplifies the testing necessary for obtaining the static modulus-a dependent variable in all cases. Some equations obtained for the metamorphic rocks were not considered in this study such as the work of King (1983) due to being the values of dynamic elastic modulus in a range from 40 GPa to 120 GPa. They have very high elastic

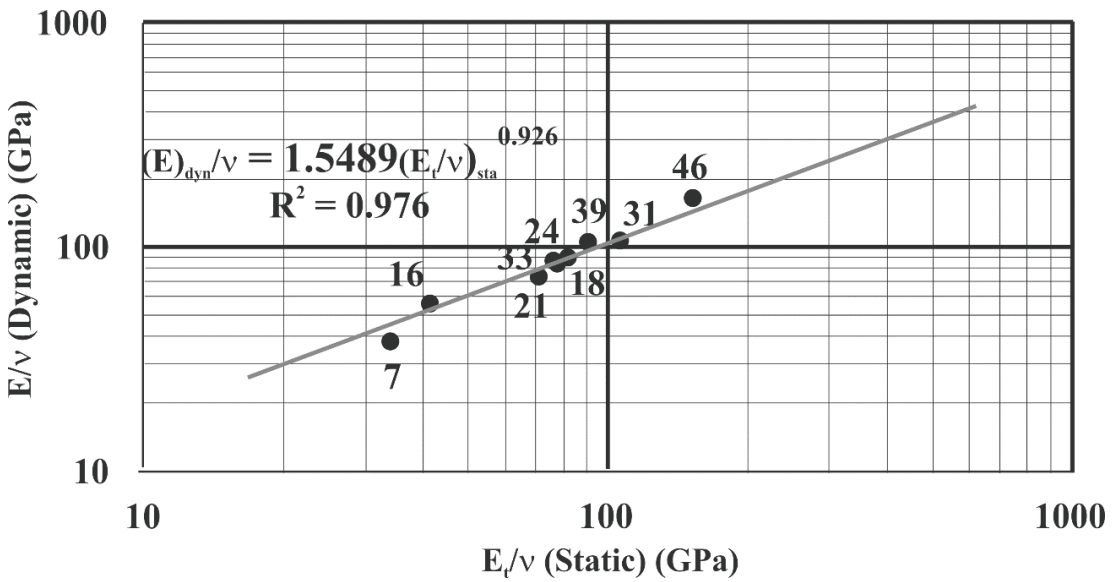

Figure 11. The plot of $(\frac{E}{\nu})_{dynamic}$ against $(\frac{E_t}{\nu})_{static}$ for the micaschists core specimens from the Burgaz dam site.

Şekil 11. Burgaz Baraj alanındaki mikaşist karot numuneleri için hazırlanmış olan $(\frac{E}{\nu})_{dynamic}$ karşı $(\frac{E_t}{\nu})_{static}$ ilişkisi.

modulus with respect to the micaschists. When considering V_p, E_{static} modulus is calculated with the help of the equations given in Table 8. These equations use Vp parameter, which hence allows the E_{sta} modulus of rocks to be estimated quickly and reliably. Excellent matching is observed in Figure 13 for the curves of Brotons et al. (2016) and the current study, and reasonable good matching for the curve of limestone of Najibi et al. (2015).

Two multiple non-linear regression analyses (Milton et al., 1997) were conducted by SPSS software in order to estimate E_{static} with regard to V_p and porosity (n%). Two expressions from the analyses are as follows; Model 1: $E_{static} = Vp^{2.523} \times n^{0.095}$, $R^2 = 0.93$, RMSE [(Root mean square error). Root mean squared error (RMSE) is the most commonly used error metric. It expresses the square root of the average squared errors of a predictive model. The model is assumed to be as excellent while RMSE is 0]: 0.149 GPa, VAF (Variance accounted for): 92.67. Model 2: $E_{static} = 8.966\ V_p \times n^{-0.753}$, $R^2 = 0.75$, RMSE: 1.80 GPa and VAF: 75.54. As a result, multiple non-linear regression model 1 estimated the E_{static} values more precisely than other models as having low RMSE (0.149) and high VAF (92.67) values.

Estimation of Settlement Potential and Bearing Capacity Value

Pressuremeter tests were performed along the ASK-1 borehole profile to determine the values of elastic modulus of micaschists rock masses with various weathering grades. Thus, the amount of settlement and bearing capacity value of micaschists both in and beneath the cutoff zone were calculated by using the values of elastic modulus of the rock masses. The weathering degree of micaschist is varying from moderately weathered to completely weathered and the rock mass is highly jointed (Figure 4 and Table 9). Pressuremeter tests were generally performed in every two meters in ASK 1 borehole between the depth 5.0 m and 53.5 m.

Table 8. The relationships between E_{static} modulus and P-wave velocity for various rock types as well as the current study.

Çizelge 8. Bu çalışmadaki mikaşistler ve farklı kaya türleri için E_{static} modülü ve P-dalga hızı ilişkileri.

Reference	Relationship	R^2	Rock type	α angle*
Najibi et al. (2015)	$E_{static} = 0.169 \times V_p^{3.324}$	0.90	Limestone	-
Brotons et al. (2016)	$E_{static} = 0.679 \times V_p^{2.664}$	0.99	All types	-
The current study	$E_{static} = 1.101 \times V_p^{2.4757}$	0.95	Mica schist	α = 90°
	$E_{static} = V_p^{2.523} \times n^{0.095}$	0.92	Mica schist	α = 90°

*: α is defined as an acute angle between the measurement direction of V_p and the schistosity plane orientation. n: Porosity values of the micaschist core specimens.

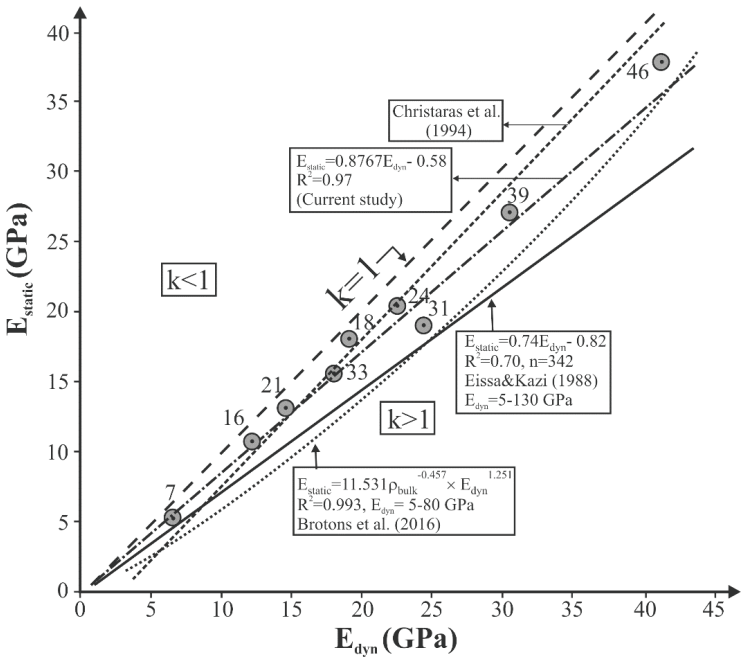

Figure 12. The plot of the relationships between static and dynamic moduli proposed by various authors and the current study (k is the dimensionless coefficient obtained from the ratio of dynamic modulus to static modulus).

Şekil 12. Bu çalışmadaki mikaşistler ve farklı yazarların önerdikleri statik ve dinamik modül arasındaki ilişkiler.

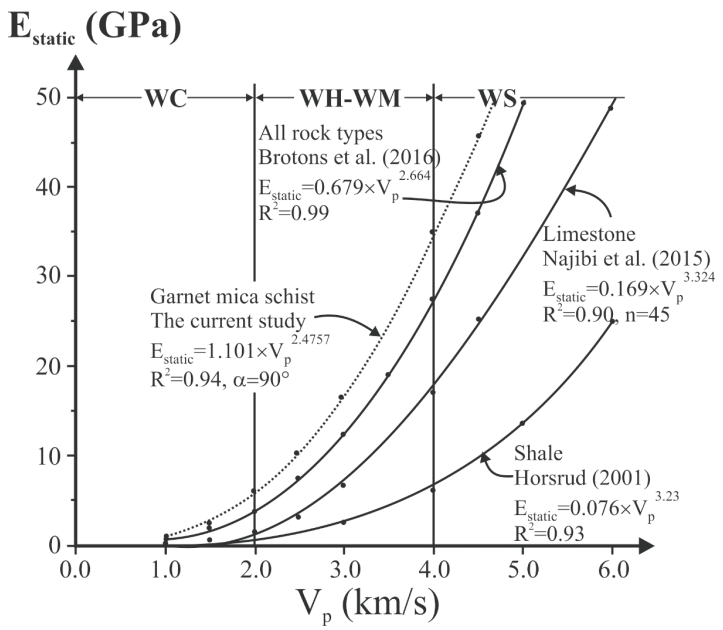

Figure 13. Variation of the static modulus (E_{static}) with the compression wave velocity (V_p) according to different authors and the current study (α: anisotropy angle).

Şekil 13. Bu çalışmadaki mikaşistler ve farklı yazarların önerdikleri statik modülün P-dalga hazına bağlı değişimi.

Table 9. Menard Pressuremeter test results for the ASK 1 borehole.

Çizelge 9. ASK-1 sondaj kuyusu için Menard Presiyometre deney sonuçları.

Zone	Depth (m)	P_L	E_M (MPa)	G_M (MPa)	E_M/P_L	Soil type and settlement (mm)
Alluvium	5.00	0.20	1.0	0.62	5.0	Firm to very firm soils
	10.0	0.30	1.9	1.23	6.3	
	15.0	0.85	1.4	0.91	7.7	
	17.0	0.50	6.6	4.16	2.8	
Zone of cutoff	21.0	0.94	9.4	5.87	9.96	Very decomposed micaschist, hard soil to weak rock (Transition zone) "Base of the dam"
	24.5	4.00	39.9	24.9	9.97	
	26.5	4.89	97.9	60.2	20.02	
	28.5	5.0	103.3	64.5	20.66	
Zone 1 The zone of bearing capacity	30.5	7.9	1220	714.9	154.4	Settlement: 2.23 mm
	31.5	8.80	1440	914.4	163.6	Harmonic mean of three E_M-values, E_M: 1398.6 MPa
	33.5	9.65	1585	935.1	164.2	Settlement: 2.16 mm
	35.5	9.95	1700	1000.3	170.8	Moderately weathered and fractured micaschists
	37.5	9.80	1752	1139.0	178.8	
More fractured zone	39.5	3.18	454.4	272.6	142.9	Moderately weathered and fractured micaschists
	41.5	3.17	520.0	312.0	164.4	
Zone 2	43.5	7.90	1340	804.0	169.6	
	45.5	9.85	1640	984.0	166.5	
	47.5	10.2	1810	1086.0	177.8	
	49.5	10.2	1830	1098.0	179.4	
	51.5	10.1	1796	1077.6	177.8	
	53.5	11.9	2150	1344.0	180.67	

G_M: Shear modulus [$E_M/2\times(1+\nu)$]. Settlement w e calculated according to the equation suggested by Menard et al. (1962) in this work.

Moderately weathered and fractured micaschists take place under both the zone of pressure bulb and the more fractured zone along the profile of ASK–1 borehole. The first part with 3 m depth of the zone 1 is the zone of bearing capacity and this zone is important in term of a foundation.

Clarke (1995) indicated that as the ratio of Menard deformation modulus to Menard limit pressure $\left(E_M/P_L\right)$ is between 10 and 20, the

soil is firm and very firm. This ratio is changing from 5.0 to 20.66 in eight pressuremeter tests performed in ASK 1 borehole between the depths 5.0 m and 28.5 m. It was determined that the thickness of the cutoff zone under the alluvium changes between 5 and 7.5 m on the basis of the core description and the results of pressuremeter tests. These results fundamentally indicate that this zone is a transition zone from hard soil to weak rock. Thirteen pressuremeter tests between the depths 30.5 m and 53.5 m were carried out and yielded Menard deformation modulus were calculated to be between 454.4 MPa and 2150 MPa with an arithmetic mean value of 1479.8 MPa and a standard deviation of 500.1 MPa. It was determined that the $\left({E_M}/{P_L}\right)$ ratio for moderately weathered and fractured micaschists varied from 142.9 to 180.67. By ignoring extremely high and low values, the range of $\left({E_M}/{P_L}\right)$ ratio varies between 154.4 to 179.4 which is still high. As a result, the ratio of $\left({E_M}/{P_L}\right)$ is quite useful and typical values are 9.96 to 20.66 in very decomposed micaschist to the extent of very dense sand (Table 9). This is a transition zone between hard soil and weak rock. On the other hand, the $\left({E_M}/{P_L}\right)$ ratio under the cutoff level (Zone I) reaches up to 142.9 to 180.67 in moderately and highly weathered, and fractured micaschists (Table 9). The aperture of fractures in the rock mass for zone 1 is changing between 1 mm and 1.5 mm and schistosity planes are nearly horizontal. In this case, variations of $\left({E_M}/{P_L}\right)$ ratios are not due to the closing of apertures during pressuremeter tests. Işık et al. (2008) observed that testing depth and disturbance affect the calculated values of the deformation modulus of greywackes. In addition, they remarked that the volume subjected to the applied pressure is small when compared to the rock mass volume. Thus, the deformation modulus of the rock mass derived from the test should be used cautiously. The effect of variable stress condition in highly fractured mica schist zone (39.5 m – 41.5 m) and testing depth were not considered in this study. Pressuremeter tests indicated that for a 115 m high dam, the settlement would vary between some 2.16 mm and 2.23 mm. The ultimate bearing capacity (q_{ult}) at the base of the dam structure was computed as ranging between 2.96 MPa and 3.71 MPa (For the zone 1: -min: 7.90 MPa and -max: 9.95 MPa, coefficient of bearing capacity, k : 1.1, unit weight: 26.5 kN/m^3, factor of safety: 3). Bearing capacity analyses were performed according to the equation suggested by Baguelin et al. (1978). After the excavation of cutoff with 7.5 m depth from alluvium at the base of river valley was performed, the dam construction was started. Weathered micaschist unit lies down at this elevation (28 m). The harmonic mean of elastic moduli for three measurements in the micaschist rock mass beneath the dam was computed as 1398.6 MPa (Table 9). Considering the harmonic mean value (E_M: 1398.6 MPa), the amount of settlement was obtained as 2.16 mm. On the other hand, if the minimum value of elastic modulus of the rock mass for a measurement (E_M: 1220 MPa) beneath the dam is considered, amount of settlement is calculated as 2.23 mm.

Relationship Between Elastic Modulus of the Micaschist Rock Mass (E_M) and Uniaxial Compressive Strength of the Micaschist Rock Material (σ_c)

Data from in-situ and laboratory tests, which was used in the establishment of the relation between E_M and σ_c, is presented in Table 10. Variation of the elastic modulus of E_M with σ_c is investigated (Figure 14). The relations given in Equations 7 and 8 are obtained by using linear and power regression analyses;

$$E_M = 0.322\sqrt{\sigma_c} - 0.606,\ R^2 = 0.95 \quad (7)$$

$$E_M = 0.1194\ (\sigma_c)^{1.3472},\ R^2 = 0.94 \quad (8)$$

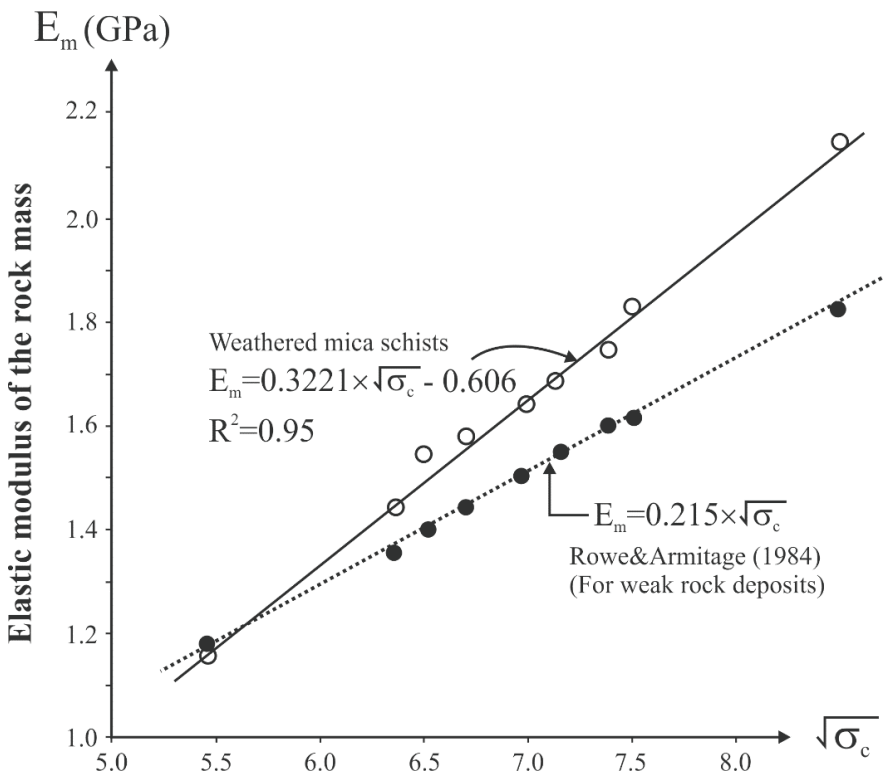

Figure 14. Variation of the elastic modulus of the micaschist rock mass with the uniaxial compressive strength of the intact rock material.

Şekil 14. Mikaşist kayaç kütlesinin elastik modülünün taze kayacın tek eksenli basınç dayanımıyla değişimi.

Table 10. Data for elastic modulus of rock mass (E_M) and UCS-values of the intact rock.

Çizelge 10. Kayaç kütlesinin elastisite modülü ve sağlam kayanın tek eksenli basınç dayanımı verileri.

E_t (GPa)	σ_c *(MPa)*	$\sqrt{\sigma_c}$	Current study E_M (GPa)	Rowe and Armitage (1984) E_M (GPa)	Palmström and Singh (2001), E_M (GPa)
5.98	29.8	5.46	1.220	1.170	5.96
10.82	42.6	6.52	1.550	1.390	8.52
13.00	48.0	6.93	1.650	1.400	9.60
15.52	40.5	6.36	1.440	1.360	8.10
17.86	51.4	7.17	1.700	1.540	10.28
19.00	55.0	7.41	1.752	1.590	11.00
20.59	45.0	6.70	1.585	1.440	9.00
27.12	56.2	7.49	1.830	1.610	11.20
36.40	71.6	8.46	2.150	1.820	14.32

The graph showing the variation of the elastic modulus of the micaschist rock mass with σ_c is presented in Figure 14. In this graph, two lines from the current study and Rowe and Armitage (1984) are compared with each other. For the low values of σ_c ($\sigma_c \geq 32$ MPa), the values of elastic modulus from both equations are quite close to each other. For the high values of σ_c, both trend lines are, however, getting distant from each other.

Comparison of In-situ and Estimated Rock Mass Deformation Moduli by Considering the RQD-Values

Coon and Merrit (1970) proposed the following equation considering the RQD values; $\frac{E_M}{E_i}$ = (0.0231× RQD) – 1.32, based on the more data and more recently Zhang and Einstein (2004) recommended the following relations considering the RQD values;

$\frac{E_M}{E_i} = 0.2 \times 10^{(0.0186 \times RQD - 1.91)}$ (Lower bound),

$\frac{E_M}{E_i} = 1.8 \times 10^{(0.0186 \times RQD - 1.91)}$ (Upper bound),

$\frac{E_M}{E_i} = 10^{(0.0186 \times RQD - 1.91)}$, $R^2 = 0.76$ (Mean), where E_M and E_i are the deformation modulus of the rock mass and intact rock, respectively.

Pressuremeter test results (E_M) performed beneath the cutoff zone (under 30.5 m) were considered in this work. Three pressuremeter tests between the depths 30.5 and 33.5 m were performed and yielded E_M-values between 1.22 GPa and 1.7 GPa with arithmetic mean value of 1.49 GPa. On the other hand, by ignoring extremely high and low values, the RQD-values in this zone generally vary between 35% and 60% with arithmetic mean value of 48.5% (Figure 4). For the RQD values of 35% and 60%, $\frac{E_M}{E_i}$ ratios are found as 0.011 (Lower bound) and 0.289 (Upper bound), respectively. The mean value (RQD: 48.5%) is found as 0.0982. At depths between 30.5 m and 33.5 m (bearing capacity zone), the values of static modulus, E_t vary between 5.98 GPa and 17.86 GPa with arithmetic mean value of 11.55 GPa (Table 5).

Lower bound; $\frac{E_M}{Ei\,(\min)} = 0.011$, $\frac{E_M}{5.98} = 0.011$; $E_M = 5.98 \times 0.011 = 0.0658$ GPa (65.8 MPa),

Upper bound; $\frac{E_M}{Ei\,(\max)} = 0.289$, $\frac{E_M}{17.86} = 0.289$; $E_M = 17.86 \times 0.289 = 5.16$ GPa (5160 MPa),

Mean; $\frac{E_M}{Ei\,(\text{mean})} = 0.0982$, $\frac{E_M}{11.55} = 0.0982$; $E_M = 11.55 \times 0.0982 = 1.134$ GPa (1134 MPa).

When the RQD-values are considered, it is understood that the lower and the upper bound values of elastic modulus of weathered micaschist rock mass vary between 65.8 MPa and 5160 MPa with arithmetic mean value of 1134 MPa. These values mentioned above are the estimated values obtained from the equations of Zhang and Einstein (2004). On the other hand, the mean ratio based on the pressuremeter test results (E_M) and laboratory deformability tests (E_i) [$E_{i(mean)} = \frac{(5.98+10.82+17.86)}{3} = 11.553$ GPa (from Table 5)] for the bearing capacity zone is as follows; Mean: $\frac{E_{M(mean)}}{E_{i(mean)}} = \frac{1490}{11553} = 0.129$. This ratio (0.129) takes part between two ratios obtained using the equations of the mean and the upper bound of Zhang and Einstein (2004). For this reason, disturbance during the drilling operations may cause the deformation modulus (E_M) obtained from Menard pressuremeter test to become lower than the actual in-situ value. When the estimated ratios considering the RQD-values and in-situ ratios based on the pressuremeter test results (E_M) and laboratory deformability tests are compared, it is seen that they are consistent with each other.

DISCUSSION

The discussions are based on the laboratory tests employed on the intact micaschist core specimens and pressuremeter tests. V_s as a percentage of V_p was calculated for the micaschists, and the results are consistent in that average V_s values are roughly 60% of V_p values (min: 57.8%, max: 64.2%, mean 61.2% for the mean porosity value of 3.55%). It was determined that the relationships between and UCS, and porosity had a good correlation with the correlation factors r = 0.81 and r = 0.88, respectively. The porosity and UCS and, $V_{p\text{-}dry}$, and $V_{p\text{-}sat}$, the UCS and $V_{p\text{-}dry}$ had even better correlations of ≥ 0.90. Empirical relationships proposed in the related literature for the parameters studied were also considered, between V_p and UCS (Table 11). The proposed equation in this work was in this work is similar to the equation proposed by the equation proposed by Andrade and Saraiva (2010).

It was determined that the micaschists located at the depth between 28.5 and 40 m had lower UCS values when compared with those of under 40 m depth (In this zone, the existence of the micaschist level with the properties of $V_{p\text{-}dry}$ < 2000 m/s and 20.3 < σ_c < 28.2 MPa were determined). This case indicated that a more weathered and fractured material exists in these depths. The depth between 28.5 m and 40 m below the dam should be considered in terms of the compaction grouting. Considering the results of the deformability tests, the micaschists were classified as "average modulus ratio and moderately strong rock" according to the classification suggested by Deere and Miller (1966). According to the method suggested by Türk and Dearman (1983), they were also classified as "moderately deformable and strong rock". It was understood that the rock material classification of the micaschists proposed by Türk and Dearman (1983) is similar to Deeres', the difference being in the division of the elastic modulus by Poisson′s ratio.

The micaschists take place beneath the cutoff level of the dam were classified as "moderate deformable rock" ($15 \times 10^3 < E_t < 30 \times 10^3$ MPa). The values of UCS of nine intact core specimens on which deformability tests were performed, were determined to be in the range between 29.8 MPa and 71.6 MPa. The mean value of UCS of all core specimens was also determined as 48.89±11.74 MPa. The values of V_{pdry} of the nine core specimens were found to be in the range between 1906 m/s and 3850 m/s. According to the information given above, except core specimen number 7, the eight core specimens were chosen from moderately weathered and "moderately strong" and "strong" micaschist core specimens that represent 78% of all core specimens. The core specimen number 7 was chosen from highly weathered and weak rock micaschist core specimens that represent 10% of all specimens.

Table 11. Equations derived from the correlations between the Vp and the UCS values.

Çizelge 11. P-dalga hızı ve tek eksenli basınç değerleri arasındaki korelasyonlardan türeyen eşitlikler.

Proposed equations of the references	Rock type	References
$UCS = 0.020\ V_{p\text{-}dry} - 10.05$	Micaschist	The current study
$UCS = 0.019\ V_{p\text{-}dry} - 1.76$	Phyllites	Andrade and Saraiva (2010)
$UCS = 0.064\ V_{p\text{-}dry} - 117.99$	Igneous and metamorphic	Sharma and Singh (2008)
$UCS = 0.0355\ V_{p\text{-}dry} - 55$	Granites	Tuğrul and Zarif (1999)

E_M values representing the micaschist rock mass were obtained from MPT. These values were used in settlement and bearing capacity analyses. In addition, the excavation depth of cutoff was determined by considering the pressuremeter test results ($E_M \leq 103.3$ MPa). It was determined that the excavation depth under alluvium changes as a range between 5 m and 7.5 m. It was also determined that the values of E_M under the cutoff zone are greater than 454.4 MPa. In addition, minimum, maximum and arithmetic mean values of Em were determined as 454.4 MPa, 2150 MPa and 1479.8 MPa, respectively. The rock mass modulus obtained from the Rock Mass Rating (RMR) tends to overestimate when compared with E_M based on MPT (Birid, 2015). Analyses indicated that the settlement for a 115 m high rockfill dam would be in the order of 2.16 mm and 2.23 mm. On the other hand, the ultimate bearing capacity of the micaschist beneath the dam were also computed as ranging between 2.96 MPa and 3.71 MPa.

The relationship between σ_c and $\frac{E_t}{\nu}$ for the Burgaz′s micaschists was determined to be as follows; $\sigma_c = 5.3936 \times \left(\frac{E_t}{\nu}\right)^{0.5047}$. As known, weathering decreases not only strength but also the ratio of elastic modulus to Poisson′s ratio. The experimental results from the micaschist weathered to different grades (*i.* Burgaz dam site, İzmir *ii.* Selçuk, Belevi, İzmir) were similarly plotted on a log-log paper. Thus, the relationship between σ_c and $\frac{E_t}{\nu}$ for both Burgaz and Selçuk′s micaschists was also determined as follows; $\sigma_c = 7.5393 \times \left(\frac{E_t}{\nu}\right)^{0.4244}$. The slope of the strength versus $\left(\frac{E_t}{\nu}\right)$ plot for a particular rock is constant so that for each rock there is a unique linear equation on a log-log scale.

The plot of $(\frac{E}{\nu})_{dynamic}$ against $(\frac{E_t}{\nu})_{static}$ for the micaschists core specimens (WM) from the Burgaz dam site was obtained. Test results gave a positive power relation of $(\frac{E}{\nu})_{dynamic} = 1.2707 (\frac{E_t}{\nu})^{0.968}_{static}$, $R^2 = 0.96$. Thus, it will be possible that the ratio of $(\frac{E_t}{\nu})_{static}$ for the micaschists in the Burgaz dam site is computed by measurements of sonic wave velocities on the intact core specimens in the laboratory. In addition, it was understood that $(\frac{E}{\nu})_{dynamic}$ is slightly higher than $(\frac{E_t}{\nu})_{static}$. This difference can be explained as the presence of fractures as well as weak schistosity planes in micaschists.

Strength reductions in dry and water saturated conditions arisen due to the anisotropy effect were found as 47.5% and 69.3% respectively. These ratios were determined as 55.1% and 75.5% by Zhang et al. (2011). The results obtained from the two works are slightly different from each other. The first reason for this may be mineralogical composition and grain size of minerals. While the ratio of mica minerals changes between 27.9 % and 48.7 % in the study published by Zhang et al. (2011), this ratio is less than 20 % in this work. As compared on the basis of mineralogical compositions, it is seen that the ratios of mica minerals are fairly different from each other. This case negatively affects the strength of the rock. In addition, high mica content in rock can be increased the anisotropy effect. Because mica flakes existing along the schistosity planes easily weather to clay minerals. This is anyway the cause of the relatively weak nature of the schistosity planes. Thus, the sliding movement along these surfaces gets easy. The second reason may be the differences in weathering grade determination of the test specimens employed to the laboratory tests. As known, the investigation of the anisotropy effect must be conducted on the core specimens with the same weathering grade.

Increasing in V_p for different α - angles obtained from the measurements taken in dry and water saturated conditions were determined as follows; for α = 0 – 3°: 17.4%, for α= 28° – 30°: 36.3% and for α= 90°: 57.3%. When P – wave propagated vertical to the schistosity planes (α= 90°), the presence of water significantly increased the velocity (increasing the velocity: 57.3%). For the P – wave propagated along the schistosity planes (α = 0 – 3°), the presence of water only occurred a light effect on the wave velocity (increasing the velocity: 17.4%). In a similar way, V_{psat}/V_{pdry} ratios were also computed for different orientation of the schistosity planes varying from 0° to 90° with respect to the loading direction. It was determined that the V_{psat}/V_{pdry} ratio was the highest for α= 90° (2.34) and the smallest for α=0°–3° (1.21), while the ratio for α= 28° – 30° was intermediate (1.57). The results obtained from the computations of the V_{psat}/V_{pdry} ratio and increasing the velocity for different α - angles agree with each other.

CONCLUSIONS

It was determined that as the degree of weathering of the micaschists increases, to ratio also increases. On the other hand, V_{psat} to V_{pdry} ratio is roughly 1.67. The proposed equation to estimate the UCS values based on the V_p values is different from the empirical equations in the related literature due to the differences relating to the mineralogy and texture of the rock materials. In order to determine the static modulus of the micaschist rock material, there are two ways proposed in this study; one of these is to utilize from E_{dyn} and another one is from V_p. The equations in relation to the static modulus were determined as follows;

$$E_{static}=0.8767 \times E_{dyn}-0.58,\ E_{static} = 1.1015 \times V_p^{2.4757},\ E_{static} = V_p^{2.523\times n^{0.095}} \quad (9)$$

It is concluded that the static modulus can be obtained from the dynamic tests, as shown in the equations for the studies range (i. e. E_{dyn} values lower than 30.5 GPa and soft rocks). Variation of the elastic modulus of the micaschist rock mass (E_M) with UCS-values was investigated and the relation given below was obtained; $E_M = 0.3221 \sqrt{\sigma_c} - 0.606$, $R^2 = 0.95$. In this work, the estimated ratios considering the RQD values (the equation of Zhang and Einstein, 2004 was used) and ($\frac{E_{MPT}}{E_i}$) ratios from this study were compared with each other. As a result, it was determined that they are quite consistent with each other. This case indicates that the elastic modulus representing the micaschist rock mass, which was used in the settlement analyses, is more suitable. It was concluded that the settlement for a 115 m high rockfill dam would be in the order of 2.23 mm. In addition, the ultimate bearing capacities of the micaschists beneath the dam were also computed as ranging between 2.96 and 3.71 MPa. It can be said that this would be a good site for the dam construction in terms of bearing capacity, amount of settlement and the deformability of the base rock beneath the dam structure.

Anisotropy effect will not occur in the bedrock beneath the cutoff level of the dam structure due to the existence of the schistosity planes with nearly horizontal position (α < 20°). It was determined that the V_p – values obtained as parallel to the schistosity planes were greater than those of other orientations in both dry and water saturated conditions. In water saturated condition, V_p–values were obtained as close to each other for α = 28°– 30° and α=90°. In dry condition, V_p–values obtained at α=28°– 30° were determined to be greater than those normal to the schistosity planes. On the other hand, It was also determined that the presence of water significantly increased the velocity (the velocity increase: 134%) when P–wave propagated as

vertical to the schistosity planes. For the P–wave propagating along the schistosity planes, it was determined that the presence of water slightly affects on the wave velocity (the velocity increase: 21.2 %). It was also determined that the highest UCS – values obtained from the UCS tests when loading is perpendicular to the schistosity planes in dry and water saturated conditions. On the other hand, the lowest ones were obtained from the tests when loading was inclined to the schistosity planes (α = 28°–30°) in similar conditions. It was determined that while the curves of stress values versus anisotropy angle (α) displayed a similar "V - shape", the curves of V_p did not display such a trend. It was also determined that the largest and smallest σ_c^d / σ_c^s ratios were found as 2.35 (for α = 28°–30°) and 1.37 (α = 90°), respectively. On the other hand, the maximum strength reductions for dry and water saturated conditions due to the anisotropy effect were computed as 47.51 % and 69.31 %, respectively.

The equation given below was obtained for the micaschist weathered to different grades; $\sigma_c = 7.5393 \times \left(\frac{E_t}{\nu}\right)^{0.4244}$, where "m" is 0.4244. The slope of line (m) for the micaschists is constant and has the characteristic of the rock. On the other hand, the relation of $(\frac{E}{\nu})_{dyn}$ versus $\left(\frac{E_t}{\nu}\right)_{static}$ for the weathered schists was found as $(\frac{E}{\nu}) = 1.2707 \, (\frac{E_t}{\nu})^{0.968}_{static}$.

REFERENCES

Al-Shayea, N.A., 2004. Effects of testing methods and conditions on the elastic properties of limestone rock. Engineering Geology, 74, 139-156.

Anon, 1979. Classification of rocks and soils for engineering geological mapping, Part 1 – Rock and soil materials. Bull. Int. Ass. Engineering Geology, 19, 364 – 371.

Anon, 1981. British Standard 5930: Site Investigations, London. British Standards Institution, pp. 147.

Andrade, P.S., Saraiva, A.A., 2010. Physical and mechanical characterization of phyllites and metagreywackes in central Portugal. Bull. Eng. Geol. Environ., 69, 207-214.

ASTM D 2845-08, 1990. Standard Test Method for Laboratory Determination of Pulse Velocities and Ultrasonic Elastic Constants of Rocks, American Society Testing Materials.

ASTM D 2938-95, 1992. Standard Test Method for Unconfined Compressive Strength of Intact Core Specimens. Rock testing handbook, 89-111.

Baguelin, F., Jézéquel, J.F., Shields, D.H., 1978. The pressuremeter and foundation engineering. Clausthal: Trans Tech Publications.

Behrestaghi, M.H.N., Rao, K.S., Ramamurhy, T., 1996. Engineering geological and geotechnical responses of schistosity rocks from dam project areas in India. Engineering Geology, 44 (1 – 4), 183 – 201.

Birid, K.C., 2015. Interpretation of pressuremeter tests in rock, ISP7-PRESSIO 2015, Frikha, Varaksin&Gambin (Eds), Conference paper, pp. 289 – 300.

Brotons, V., Tomas R., Ivorra S., Grediaga A., 2014. Relationship between static and dynamic modulus of a calcarenite heated at different temparatures: the San Julian′s stone. Bull. Eng. Geol. Environ, 73, 791–799.

Brotons, V., Tomas R., Ivorra S., Grediaga A., Martinez T.M., 2016. Improved correlation between the static and dynamic elastic modulus of different types of rocks. Material and Structures, 49, 3021 – 3027.

Christaras, B., Auger, F., Mosse, E., 1994. Determination of the moduli of elasticity of rocks. Comparison of the ultrasonic velocity and mechanical resonance frequency methods with direct static methods. Materials and Structures, 27, 222–228.

Chang, C.D., Zoback, M.D., Khaksar, A., 2006. Empirical relations between rock strength and physical properties in sedimentary rocks. Journal of Petroleum Science and Engineering, 51 (3-4), 223-237.

Clarke, B.G., 1995. Pressuremeters in geotechnical design. Blackie Academic and Professional, Chapman and Hall, London.

Coon, R.F., Merritt, A.H., 1970. Predicting in-situ modulus of deformation using rock quality indices. Determination of Rock, ASTM STP, 477, 154 – 175.

Deere, D.U., Miller, R.P., 1966. Engineering classification and index properties for intact rock, Report AFML-TR-65-116. Air Force Weapons Laboratory (WLDC) Kirtland Air Force Base, New Mexico, 87117.

Eissa, E.A., Kazi, A., 1988. Relation between static and dynamic Young′s Moduli of rocks. International Journal of Rock Mechanics and Mining Science Geomechanics Abstracts, 25, (6), 479–482.

Elçi, H., 2003. Engineering Geology of Selçuk Town, Izmir, Master of degree science, Ms Thesis, Dokuz Eylul University, İzmir-Turkey, p. 208.

Entwisle, D.C., Hobbs, P.R.N., Jones, L.D., Guuss, D., Raines, M.G., 2005. The relation between effective porosity, uniaxial compressive strength and sonic velocity of intact Borrowdale Volcanic Group core samples from Sellafield. Geotech. Geol. Eng., 23, 793-809.

Gardner, W.S., 1987. Design of drilled piers in the Atlantic Piedmont. Smith R. E. editor. Design", M. Te′eni, Ed., Wiley-Interscience, New York (1971), Part 2, p. 1379-1404.

Gupta, A.S., Seshagiri, R.K., 1998. Index properties of weathered rocks: inter-relationships and applicability. Bull. Eng. Geol. Env., 57, 161 – 172.

Heap, M.J., Lavalice, Y., Petrakova, L., Baud, P., Reuschle, T., Varley, N.R., Dingwell, D.B., 2014. Microstructural controls on the physical and mechanical properties of edifice-forming andesites at Volcan de Colima. Mex. J. Geophys Res. Solid Earth, 119, 2925–2963.

Horsrud, P., 2001. Estimating mechanical properties of shale from empirical correlations. SPE Drilling&Completion, 16 (2), 68-73.

Hughes, J., 2002. Use of pressuremeter in weak rocks of the lower Nanaimo Series. Proceedings of 16th Annual Vancouver Geotech. Soc. Symp. on Foundation Eng., 29 – 30.

Işık, N.S., Ulusay, R., Doyuran, V., 2008. Deformation modulus of heavily jointed-sheared and block greywackes by pressuremeter tests: Numerical, experimental and empirical assessments. Eng. Geo., 101, 269 – 282.

Kadakçı Koca, T., Koca, M.Y., 2018. Classification of weathered andesitic rock materials from the Izmir Subway line on the basis of strength and deformation. Bull. of Eng. Geol. and the Environ., doi.org/10.1007/s10064-018-1346-y.

Kayabasi, A., Gokceoglu, C., Ercanoglu, M., 2003. Estimating the deformation modulus of rock masses: a comparative study. International Journal of Rock Mechanics and Mining Science40, 55 – 63.

Kıncal, C., Koca, M.Y., 2019. Correlations of in-situ modulus of deformation with elastic modulus of intact core specimens and RMR values of andesitic rocks: a case study of the İzmir subway line, Bull. Eng. Geol. and the Environ., doi. org/10.1007/s10064-018-01443-5.

King, M.S., 1983. Static and dynamic elastic properties of rocks from the Canadian shield. International Journal of Rock Mechanics and Mining Science, 20, 237–241.

Lama, R.D., Vutukuri, V.S., 1978. Handbook on Mechanical Properties of Rocks-Testing Techniques and Results, 11, p. 481. Trans. Tech. Publications, Clauthal, Germany.

Mc Cann, D.M., Culshaw, M.G., Northmore, K., 1990. Rock mass assessment from seismic measurements, In Field Testing in Engineering Geology, F. G. Bell, M. G. Culshaw, J. C. Cripps and J. B. Coffey (eds.) Engineering Special Publication, No. 6, Geological Society, London, pp. 257 – 266.

Menard, L., 1975. Interpretation and application of pressuremeter tests results to foundations design (D60). Sols Soils No. 26, Paris.

Menard, L., Rousseau, J., 1962. L'evaluation des tassements. Tendances nouvelles. Sols Soils No. 1, pp. 13-20, Paris.

Milton, J.S., McTeer, P.M., Corbet, J.J., 1997. Introduction to Statistics, McGraw and Hill Company.

Najibi, A.R., Ghafoori, M., Lashkaripour, G.R., 2015. Empirical relations between strength and static and dynamic elastic properties of Asmari and Sarvak limestones, two main oil reservoirs in Iran. J. Pet. Sci. Eng., 126, 78 – 82.

Nasseri, M.H.B., Rao, K.S., Ramamurthy, T., 2003. Anisotropic strength and deformational behavior of Himalayan schists. International Journal of Rock Mechanics and Mining Science, 40 (1), 3–23.

Sharma, P.K., Singh, T.N., 2008. A correlation between P-wave velocity, impact strength index, slake durability index and uniaxial compressive strength. Bull. Eng. Geol. Environ., 67, 17-22.

Singh, V.K., Singh, D., Singh, T.N., 2001. Prediction of strength properties of some schistosity rocks from petrographic properties using artificial neural networks. International Journal of Rock Mechanics and Mining Science, 38 (2), 269 – 284.

Tarnawski, M., 2004. The Perfect Menard pressuremeter Curve. Archives of Hydro-Eng. and Environmental Mechanics, 15 (4), 387–402.

Türk, N., Dearman, W.R., 1983. A practical classification of rocks for engineering purposes. Bull. Int. Assoc. of Eng. Geo., 28, 162-167.

Tuğrul, A., Zarif, I.H., 1999. Correlation of mineralogical and textural characteristics with engineering properties of selected granitic rocks from Turkey. Engineering Geology, 51, 303-317.

Uslu, S., 2017. Engineering Geology of a Rock Slope Located in Right Bank of the Burgaz Dam Site, İzmir, Master of degree science, Ms Thesis, Dokuz Eylul University, İzmir, p. 104.

Vanheerden, W.L., 1987. General relations between static and dynamic moduli of rocks. International Journal of Rock Mechanics and Mining Science, 24, 381–385.

Zhang, L., Einstein, H.H., 2004. Using RQD to estimate the deformation modulus of rock masses.International Journal of Rock Mechanics and Mining Science, 41, 337–341.

Zhang, X.P., Wong, L.N.Y., Wang, S.J., Han, G.Y., 2011. Engineering properties of quartz mica schist. Engineering Geology 121, 135–149.